Characterization and quantification of necrotic tissues and morphology in multicellular ovarian cancer tumor spheroids using optical coherence tomography: supplement

FENG YAN,[1,4] GOKHAN GUNAY,[1,4] TRISHA I. VALERIO,[1,4] CHEN WANG,[1] JAYLA A. WILSON,[1] MAJOOD S. HADDAD,[1] MAEGAN WATSON,[1] MICHAEL O. CONNELL,[1] NOAH DAVIDSON,[1] KAR-MING FUNG,[2,3] HANDAN ACAR,[1,3,5] AND QINGGONG TANG[1,3,6]

[1]*Stephenson School of Biomedical Engineering, University of Oklahoma, OK 73019, USA*
[2]*Department of Pathology, The University of Oklahoma Health Sciences Center, Oklahoma City 73104, USA*
[3]*Stephenson Cancer Center, The University of Oklahoma Health Sciences Center, Oklahoma City 73104, USA*
[4]*Equal contribution*
[5]*hacar@ou.edu*
[6]*qtang@ou.edu*

Supplement document

Characterization and Quantification of Necrotic Tissues and Morphology in Multicellular Ovarian Cancer Tumor Spheroids Using Optical Coherence Tomography

Table S1. Comparison of manual and automatic measurements, and reproducibility measurement for four manual raters assigned cross-sectional OCT images. MAE, Sørensen-Dice similarity coefficient, and Cohen's Kappa coefficient were calculated for evaluation in quantifiable tumor regions. Reproducibility of manual quantification in tumor regions among raters was exhibited as intra-Rater reproducibility. Comparison between automatic and manual measurements was shown as Performance versus Automatic Measurement.

	Intra-Rater Reproducibility				Performance versus Automatic Measurement			
	MAE	Dice	Kappa	Kappa at >5%	MAE	Dice	Kappa	Kappa at >5%
Rater-1	28237.4	0.99	0.99	0.99	12281.6	0.94	0.86	0.87
Rater-2	30205.1	0.98	0.97	0.98	46161.6	0.94	0.86	0.89
Rater-3	17529.5	0.99	0.98	0.99	23659.5	0.95	0.86	0.89
Rater-4	19496.5	0.99	0.97	0.99	10220.5	0.94	0.85	0.91

Table S2. Data statistics and analysis of the tumor spheroids volume in 5,000- and 50,000-cells over 18 days based on voxel-counting and two diameter-based methods. M, mean, Str, standard error, $P\text{-}v1$, p-value of voxel-counting vs. diameter-based (d^3), $P\text{-}v2$, p-value of voxel-counting vs. diameter-based (w^2l), $P\text{-}v3$, p-value of diameter-based (d^3) vs. diameter-based (w^2l). $V\text{-}C$, voxel-counting, $D\text{-}D$, diameter-based. $P\text{-}STT$, paired student t-test. NS, no significant difference, *, $p\text{-value} < 0.05$, **, $p\text{-value} < 0.01$, ***, $p\text{-value} < 0.001$.

Day	M (V-C)	Str (V-C)	M (D-D d^3)	Str (D-D d^3)	M (D-D w^2l)	Str (D-D w^2l)	P-v1	P-v2	P-v3	M (V-C)	Str (V-C)	M (D-D d^3)	Str (D-D d^3)	M (D-D w^2l)	Str (D-D w^2l)	P-v1	P-v2	P-v3
D-8	2.12E+08	1.31E+07	1.36E+08	1.77E+07	1.75E+08	1.33E+07	***	***	*	3.36E+08	3.19E+07	2.81E+08	4.28E+07	3.12E+08	3.47E+07	*	*	NS
D-9	2.51E+08	2.12E+07	1.56E+08	1.64E+07	2.04E+08	1.53E+07	***	***	***	3.53E+08	1.88E+07	2.54E+08	3.19E+07	2.98E+08	2.46E+07	***	***	***
D-10	2.63E+08	3.51E+07	1.50E+08	2.39E+07	2.19E+08	2.81E+07	***	***	***	3.78E+08	1.37E+07	2.22E+08	3.11E+07	2.73E+08	2.72E+07	**	**	***
D-11	2.32E+08	6.81E+06	1.95E+08	6.73E+06	2.06E+08	7.25E+06	***	***	***	4.80E+08	9.19E+06	3.69E+08	3.86E+07	4.05E+08	2.44E+07	*	NS	**
D-12	2.53E+08	2.59E+07	2.22E+08	2.75E+07	2.26E+08	2.07E+07	***	***	***	5.39E+08	2.09E+07	4.41E+08	8.83E+07	4.17E+08	5.28E+07	***	**	***
D-13	2.73E+08	8.95E+06	2.85E+08	3.84E+07	2.86E+08	2.02E+07	***	***	***	5.26E+08	2.44E+07	4.22E+08	1.44E+08	3.98E+08	3.28E+07	***	***	***
D-14	2.66E+08	2.46E+07	1.85E+08	2.78E+07	2.13E+08	2.17E+07	***	***	***	5.26E+08	9.70E+06	4.62E+08	2.73E+07	4.47E+08	2.02E+07	***	***	***
D-15	3.30E+08	2.50E+07	2.81E+08	2.56E+07	2.91E+08	1.98E+07	***	***	***	5.29E+08	1.78E+07	4.20E+08	1.55E+07	4.62E+08	2.25E+07	***	***	***
D-16	3.57E+08	2.89E+07	2.91E+08	3.10E+07	3.12E+08	2.93E+07	***	***	***	4.55E+08	1.52E+07	3.44E+08	3.68E+06	3.98E+08	1.67E+07	***	***	*
D-17	3.44E+08	2.18E+07	2.88E+08	4.84E+07	3.10E+08	2.90E+07	**	***	NS	4.84E+08	1.89E+07	3.54E+08	3.32E+07	4.16E+08	3.58E+07	**	***	***
D-18	3.63E+08	2.18E+07	3.11E+08	2.11E+07	3.28E+08	2.17E+07	NS	***	***	4.59E+08	1.60E+07	3.58E+08	2.56E+06	3.93E+08	1.52E+07	**	***	**

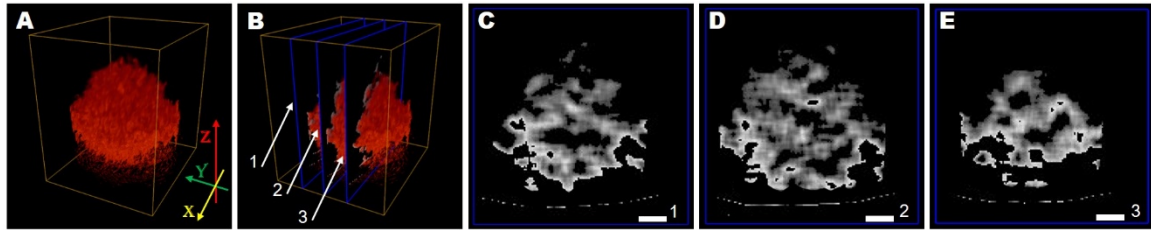|			D-1	D-2	D-3	D-4	D-5	D-6	D-7
5,000 Cell	V-C	*M*	6.24E+07	5.21E+07	7.34E+07	1.24E+08	1.29E+08	2.11E+08	2.45E+08
		Str	3.81E+06	2.24E+06	6.50E+06	5.94E+06	6.75E+06	1.72E+07	2.03E+07
	D-D (d3)	*M*	6.19E+07	3.60E+07	5.14E+07	8.20E+07	7.76E+07	1.37E+08	1.74E+08
		Str	1.40E+07	8.60E+06	5.89E+06	9.69E+06	6.11E+06	2.11E+07	2.38E+07
	D-D (w2l)	*M*	3.17E+07	4.10E+07	5.74E+07	1.03E+08	1.07E+08	1.71E+08	1.98E+08
		Str	6.45E+06	3.69E+06	4.95E+06	9.08E+06	6.02E+06	2.07E+07	1.70E+07
	P-STT	*P-v1*	***	*	***	***	***	*NS*	***
		P-v2	**	***	***	**	***	*NS*	***
		P-v3	*	*NS*	*NS*	*NS*	**	*NS*	*NS*
50,000 Cell	V-C	*M*	3.02E+08	2.50E+08	1.77E+08	1.97E+08	2.11E+08	2.29E+08	2.46E+08
		Str	2.53E+07	1.29E+07	1.10E+07	1.42E+07	9.51E+06	9.77E+06	2.07E+07
	D-D (d3)	*M*	5.97E+08	2.95E+08	1.45E+08	1.43E+08	1.43E+08	1.56E+08	1.70E+08
		Str	1.81E+08	3.71E+07	1.22E+07	1.13E+07	7.41E+06	1.42E+07	2.68E+07
	SD-D (w2l)	*M*	1.68E+08	1.65E+08	1.58E+08	1.67E+08	1.79E+08	1.95E+08	2.07E+08
		Str	1.77E+07	1.59E+07	1.18E+07	7.31E+06	7.77E+06	1.21E+07	2.62E+07
	P-STT	*P-v1*	**	**	**	***	*	*NS*	*NS*
		P-v2	*	*	***	**	*	**	*
		P-v3	*	*	*	*	*NS*	*NS*	*NS*

Figure S1

Fig. S1. 3D structure and 2D structure of necrosis core. (A) 3D structure of necrosis. (B) 3-slices (*XZ*) within the volumetric necrosis core along Y-direction. $X \times Y \times Z = 0.8 \times 0.8 \times 1.0$ mm^3. (C-E) 2D cross-sectional images of necrosis core in 75th, 125th, and 175th-slice, respectively. *Scale bar* = 100 µm.